

*Interstellar Matter and Star Formation:  
A Multi-wavelength Perspective*  
ASI Conference Series, 2010, Vol. 1, pp 135–139  
Edited by D. K. Ojha

## Young stars and protostellar cores near NGC 2023

B. Mookerjee<sup>1\*</sup>, G. Sandell<sup>2</sup>, T. H. Jarrett<sup>3</sup> and J. McMullin<sup>4</sup>

<sup>1</sup>*Tata Institute of Fundamental Research, Mumbai 400 005, India*

<sup>2</sup>*SOFIA-USRA, NASA Ames Research Center, MS 211-3, Moffett Field, CA 94035, USA*

<sup>3</sup>*Spitzer Science Center, California Institute of Technology, Pasadena, CA, 91125, USA*

<sup>4</sup>*Joint ALMA Observatory, Av Apoquindo 3650 Piso 18, Las Condes, Santiago, Chile &  
The National Radio Astronomy Observatory, 520 Edgemont Road Charlottesville,  
VA 22903-2475, USA*

**Abstract.** We present the results of our investigation of the young (proto)stellar population in NGC 2023 and the L 1630 molecular cloud bordering the H II region IC 434, using Spitzer IRAC and MIPS archive data and JCMT SCUBA imaging. We have performed photometry of all IRAC and MIPS images, and used colour-colour diagrams to identify and classify all young stars seen within a  $22' \times 26'$  field along the boundary between IC 434 and L 1630. We identify a total of 95 mid-infrared sources and 5 sub-millimeter cores in our 850 and 450  $\mu\text{m}$  SCUBA images, two (MM 1 and MM 3) of which have embedded class 0 or I protostars. We find that HD 37903 is the most massive member of a cluster with 20 – 30 PMS stars. We also find smaller groups of PMS stars formed in the Horsehead nebula and another elephant trunk structure to the north of the Horsehead. Our study shows that the expansion of the IC 434 H II region has triggered star formation in some of the dense elephant trunk structures and compressed gas inside the L 1630 molecular cloud.

*Keywords :* ISM: clouds - ISM: dust, extinction - ISM: H II regions  
- stars: formation - stars: pre-main sequence

---

\*e-mail: bhaswati@tifr.res.in

## 1. Introduction

The southern part of the Orion B giant molecular cloud complex, L 1630, borders the large H II region IC 434, which is expanding into the molecular cloud and possibly triggering star formation. The interface between the molecular cloud and the H II region is seen as a bright north-south ridge of glowing gas with the Horsehead nebula (B33) and several smaller “elephant trunks” seen in silhouette against the bright nebulosity. B33 points directly towards the binary system,  $\sigma$  Ori, which is ionizing the H II region IC 434 (Abergel et al. 2002; Pound Reipurth & Bally). The first systematic search for dense cores and embedded star clusters in the L 1630 cloud complex was carried out by Lada, Bally & Stark (1991); Lada et al. (1991), who surveyed 3.6 square degrees in CS  $J = 2 \rightarrow 1$  (98 GHz) and in K-band ( $2.2 \mu\text{m}$ ) down to 14 mag. They identified 4 embedded clusters, the richest being associated with NGC 2024 with over 300 embedded stars, and the poorest associated with NGC 2023, a reflection nebula just north of the Horsehead with only 21 embedded sources. We adopt the distance to the source to be 400 pc in our study of the region around NGC 2023 and the Horsehead nebula. Detection of several signposts of star formation in the vicinity of NGC 2023 without any obvious optical or near-IR counterparts suggests the presence of a more embedded population of protostars hidden in the dense molecular cloud cores surrounding NGC 2023. This motivates the present work.

## 2. Mid-infrared & submillimeter photometry

We extracted observations from the Spitzer Space Observatory archive (Program ID 43: an IRAC Survey of the L1630 and L1641 (Orion) Molecular Clouds – Fazio et al. and Program ID 47: A MIPS Survey of the Orion L1641 and L1630 Molecular Clouds – Fazio et al.). We carried out multiframe PSF photometry using the SSC-developed tool APEX on all the *Spitzer* IRAC images and on the MIPS  $24 \mu\text{m}$  images. Since we are mainly interested in young stellar objects, we took the 95 sources detected in the short integration IRAC  $8 \mu\text{m}$  images as the primary list. We cross-correlated this list with sources detected in other IRAC and MIPS bands, and also with 2MASS point sources. Additionally we identify 638 additional sources, detected in both the 3.6 and  $4.5 \mu\text{m}$  wavebands. Of these sources 443 are found to have 2MASS point sources associated with them. Out of the 44 sources detected at  $24 \mu\text{m}$ , 10 were detected neither in the IRAC bands nor in the sub-millimeter images.

We obtained several large scan maps ( $8' \times 8'$ ) of the NGC 2023 region with the Submillimeter Common User Bolometer Array (SCUBA) (Holland et al. 1999) on JCMT and observed several long integration jiggle maps of the NGC 2023 MM 1/MM 2 field in December 1997. These maps were reduced

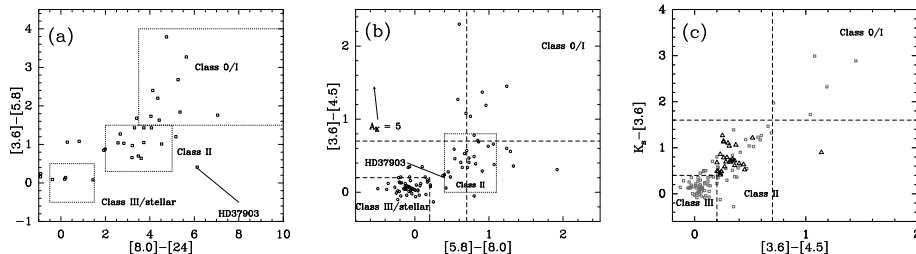


**Figure 1.** Colour-colour diagrams for all MIR and PMS-NIR sources. Approximate classification criteria adopted from Megeath et al. (2004) and Muzerolle et al. (2004) are shown respectively for the left and the middle panel. Reddening vector corresponding to the extinction laws for NGC2023/2024 given by Flaherty et al. (2007) is shown in (b). Squares and triangles in (c) correspond to sources with and without detection at  $8 \mu\text{m}$  respectively.

separately and added to earlier jiggle maps discussed in Sandell et al. (1999). The rms noise level in the final scan maps is  $45 \text{ mJy beam}^{-1}$  for the the  $850 \mu\text{m}$  map, and  $\sim 0.45 \text{ Jy beam}^{-1}$  for the  $450 \mu\text{m}$  map. The rms noise level in the jiggle maps is  $30 \text{ mJy beam}^{-1}$  at  $850 \mu\text{m}$  and  $0.23 \text{ Jy beam}^{-1}$  at  $450 \mu\text{m}$ . We have identified a total of five sub-millimeter continuum sources in the region mapped with SCUBA. These are the three sources MM 1, MM 2 and MM 5, located in the ridge (extended along north-south) lying to the west of NGC 2023 and the sources MM 3 and MM 4 located directly to the south and the south-east of the NGC 2023 nebula. With the exception of MM 3 none of the sub-mm sources is detected in the MIR band.

### 3. NIR-MIR colours & classification of YSOs

We classified the sources detected in the NGC 2023/L 1630 region using the NIR and MIR photometric data presented above. Figure 1 presents the colour-colour diagrams derived from the 2MASS, IRAC and MIPS  $24 \mu\text{m}$  magnitudes of sources detected in NGC 2023 along with several criteria (shown as dashed lines in Fig. 1) used to classify them. The colour-colour diagrams used here are suitable for distinguishing between Class 0/I and Class I protostars as well as Class II and Class III protostars. It is however not possible to distinguish the Class 0 protostars from the Class I using the MIR colours. In the  $K_s$ -[3.6] versus [3.6]-[4.5] colour-colour plot (Fig. 1 right), we also show 31 sources (out of the 443 sources detected in the 3.6 and  $4.5 \mu\text{m}$  IRAC images and with 2MASS associations) which are identified to be PMS in nature based on the colour criteria. Out of the 95 sources detected in the IRAC  $8 \mu\text{m}$  band 32 stars are found to be PMS stars (Classes I, II and I/II) based on their colours. The 10 MIPS-only sources are likely to be PMS stars. Use of the more sensitive long integration 3.6 and  $4.5 \mu\text{m}$  images in combination with 2MASS data yields

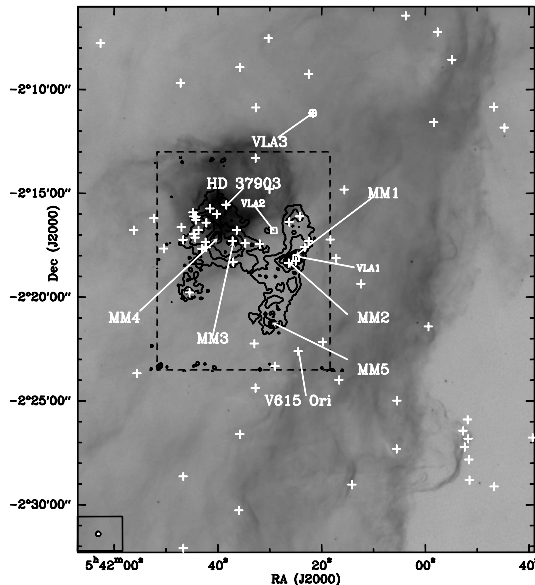


**Figure 2.** SCUBA 850  $\mu\text{m}$  contours of the entire mapped region near NGC 2023 overlaid on the Spitzer IRAC 8  $\mu\text{m}$  map image. The peak 850  $\mu\text{m}$  flux is 3.23 Jy/beam and the contours are at 0.22, 0.5, 0.75, 1.1, 1.5, 2, 2.5 and 3 Jy/beam. The beam at 850  $\mu\text{m}$  is shown at the left bottom corner. The crosses indicate the location of the sources identified as pre-main sequence objects in Fig. 1, as well as the sources not detected at 8  $\mu\text{m}$ , but identified as PMS objects from the NIR-MIR. The open square denote the location of the free-free emission sources VLA 1–3 (Reipurth et al. 2004).

an additional 31 PMS objects. Using the colour criterion,  $[3.6]-[4.5] \geq 0.2$ , for sources detected only in 3.6 and 4.5  $\mu\text{m}$  which have no 2MASS counterparts, we find another 38 sources which are likely to be PMS stars. Figure 2 shows the PMS objects identified in the region with vertical white crosses. Thus in the NGC 2023 region we identify 73 out of a total of 739 sources (111, if we include the very red sources seen only in the IRAC 3.6 and 4.5  $\mu\text{m}$  images) to be PMS in nature and of these, five are bona fide Class I sources and nine sources are identified as Class I/II.

#### 4. The YSO population in L1630

The strong concentration of Class I/0 sources near NGC 2023 suggests that this is where the youngest stars are and where star formation may still be going on. Our study re-enforces the view that a large H II region like IC 434 expanding into dense surrounding cloud complexes triggers the formation of new stars. The densest regions in the surrounding molecular clouds, like the Horsehead nebula, can even form small clusters. The pre-shock from the H II

region can compress molecular gas even further into the cloud and trigger another wave of star formation. This is demonstrated by all the young stars we find in submillimeter ridge, which runs parallel to the IC 434 boundary, but almost 0.8 pc from the edge of IC 434. Depoy et al. (1990) had estimated a total of 50 members in the young star cluster associated with NGC 2023, which has HD 37903 as its most massive member. Their estimate was based on the assumption that even a small cluster follows a Salpeter or Miller & Scalo IMF, interstellar mass function (Miller & Scalo 1979). Although we have substantially enhanced the number of YSOs in this star cluster, still, our estimate of  $\sim 32$  or possibly as few as 22 is short of the estimate by Depoy et al. (1990).

## References

- Abergel A., Bernard J. P., Boulanger F., et al., 2002, *A&A*, 389, 239  
Depoy D. L., Lada E. A., Gatley I., & Probst R., 1990, *ApJ*, 356, L55  
Flaherty K. M., Pipher J. L., Megeath S. T., et al., 2007, *ApJ*, 663, 1069  
Holland W. S., Robson E. I., Gear W. K., et al., 1999, *MNRAS*, 303, 659  
Lada E. A., Bally J., & Stark A. A., 1991, *ApJ*, 368, 432  
Lada E. A., DePoy D. L., Evans II N. J., & Gatley I., 1991, *ApJ*, 371, 171  
Megeath S. T., Allen L. E., Gutermuth R. A., et al., 2004, *ApJS*, 154, 367  
Miller E., & Scalo J. M., 1979, *ApJS*, 41, 513  
Muzerolle J., Megeath S. T., Gutermuth R. A., et al., 2004, *ApJS*, 154, 379  
Pound M. W., Reipurth B., & Bally J., 2003, *AJ*, 125, 2108  
Reipurth B., Rodríguez L. F., Anglada L., & Bally J., 2004, *AJ*, 127, 1736  
Sandell G., Avery L. W., Baas F., et al., 1999, *ApJ*, 519, 236